THE JOURNAL OF BIOLOGICAL CHEMISTRY VOL. 288, NO. 25, pp. 18058–18067, June 21, 2013


# Sec62 Protein Mediates Membrane Insertion and Orientation of Moderately Hydrophobic Signal Anchor Proteins in the Endoplasmic Reticulum (ER)*

Received for publication, March 28, 2013, and in revised form, April 23, 2013 Published, JBC Papers in Press, April 30, 2013, DOI 10.1074/jbc.M113.473009

**Johannes H. Reithinger**[‡§], **Ji Eun Hani Kim**[‡], **and Hyun Kim**[‡1]

*From the* [‡]*School of Biological Sciences, Seoul National University, Seoul 151-747, Korea and the* [§]*Center for Biomembrane Research, Department of Biochemistry and Biophysics, Stockholm University, SE-106 91 Stockholm, Sweden*

**Background:** Sec62 is an essential component of the post-translational translocation machinery in the ER.
**Results:** Translocation of moderately hydrophobic signal anchor proteins is decreased in Sec62-defective yeast cells.
**Conclusion:** Sec62 mediates membrane insertion of signal anchor proteins in the $N_{in}$-$C_{out}$ membrane orientation.
**Significance:** Sec62 plays a role in regulating membrane topogenesis of moderately hydrophobic signal anchor proteins.

**Nascent chains are known to be targeted to the endoplasmic reticulum membrane either by a signal recognition particle (SRP)-dependent co-translational or by an SRP-independent post-translational translocation route depending on signal sequences. Using a set of model and cellular proteins carrying an N-terminal signal anchor sequence of controlled hydrophobicity and yeast mutant strains defective in SRP or Sec62 function, the hydrophobicity-dependent targeting efficiency and targeting pathway preference were systematically evaluated. Our results suggest that an SRP-dependent co-translational and an SRP-independent post-translational translocation are not mutually exclusive for signal anchor proteins and that moderately hydrophobic ones require both SRP and Sec62 for proper targeting and translocation to the endoplasmic reticulum. Further, defect in Sec62 selectively reduced signal sequences inserted in an $N_{in}$-$C_{out}$ (type II) membrane topology, implying an undiscovered role of Sec62 in regulating the orientation of the signal sequence in an early stage of translocation.**

Proteins destined to subcellular organelles in the secretory pathway have either a cleavable or an uncleavable signal sequence (signal anchor sequence) in the N terminus that targets them to the endoplasmic reticulum (ER).[2] Once the signal sequence emerges from the ribosome, it is recognized by the signal recognition particle (SRP). The SRP targets the ribosome-nascent chain complex to the SRP receptor in the ER membrane. Subsequently, the ribosome-nascent chain complex is transferred to the Sec61 or Ssh1 translocon, and translocation and membrane insertion proceed (1).

In some cases, proteins are fully synthesized in the cytoplasm and post-translationally targeted to the ER. In yeast, post-translational translocation requires cytosolic chaperones, the Sec61 complex plus the Sec62/63 complex, consisting of Sec63p, Sec62p, Sec71p, and Sec72p subunits, and ER luminal chaperones such as Bip/Kar2p (2, 3). Post-translational translocation occurs also in mammalian cells for smaller proteins (4), but the mechanism is not well understood. Sec62 and Sec63 are conserved throughout all eukaryotes (5, 6). Recently, the Sec62 has been found to interact with the ribosome, suggesting its role in co-translational translocation in mammalian cells (7).

Examining targeting routes of secretory proteins in yeast, an earlier study by Ng *et al.* (8) showed that the proteins taking the SRP-dependent co-translational pathway tend to have more hydrophobic signal sequences than those taking the post-translational pathway. A similar phenomenon was also observed in *Escherichia coli* (9). In the present study, the hydrophobicity-dependent targeting efficiency and targeting pathway preference were systematically evaluated using a set of model and cellular proteins carrying a signal anchor sequence of varying hydrophobicity and yeast mutant strains defective in SRP or Sec62 function.

Our data show that defective SRP impaired targeting and translocation of signal anchor proteins of all hydrophobicity, but defect in Sec62 impaired moderately hydrophobic signal sequences only, suggesting that moderately hydrophobic signal sequences require both SRP and Sec62 for proper targeting and translocation. Further, defective Sec62 selectively reduced a fraction of signal sequences inserted as $N_{in}$-$C_{out}$ membrane topology, suggesting that the Sec62 mediates the orientation of the signal anchor sequence in an early stage of translocation.

## EXPERIMENTAL PROCEDURES

*Yeast Strains*—The haploid yeast strain BWY46 corresponds to W303-1α (*MATα*, *ade2*, *can1*, *his3*, *leu2*, *trp1*, *ura3*) (10). BWY497 (*MATa*, *sec62-1*, *ade2*, *can1*, *his3*, *leu2*, *trp1*, *ura3*) and BWY500 (*MATα*, *sec65-1*, *ade2*, *can1*, *his3*, *leu2*, *trp1*, *ura3*) are isogenic strains to W303-1α (10). Leader peptidase

* This work was supported by Basic Research Grant 2012-0001935 and Global Research Network Grant C00048 from the National Research Foundation of Korea (to H. K.).

[1] To whom correspondence should be addressed: School of Biological Sciences, Bldg. 504-421, Seoul National University, Seoul 151-747, Korea. Tel.: 82-2-880-4440; Fax: 82-2-872-1993; E-mail: joy@snu.ac.kr.

[2] The abbreviations used are: ER, endoplasmic reticulum; SRP, signal recognition particle; Dap2, dipeptidyl aminopeptidase B; Endo H, endoglycosidase H; H-segment, hydrophobic segment; IP, immunoprecipitation; Lep, leader peptidase; Pho8, repressible alkaline phosphatase; Spc3, signal peptidase complex 3; TM, transmembrane; ppαF, prepro-α-factor; DMSO, dimethyl sulfoxide; 0G, unglycosylated product; 1G, singly glycosylated product; 2G, doubly glycosylated product; DT, dual topology; gGFP, glycosylatable GFP.

(Lep) model protein was expressed in the *pdr5*Δ (*MATa*; *pdr5*Δ; *his3*Δ *1*; *leu2*Δ *0; met15*Δ *0; ura3*Δ *0*) strain (EUROSCARF).

*Model Proteins*—All plasmids were constructed from p424GPDHA (11) by overlap PCR (12) and homologous recombination (13). To construct plasmids encoding the H1 model protein with 1L/18A-7L/12A,[3] DNA fragments were amplified by PCR using plasmids used in Ref. 11 as templates, and two primers, 5′-CCCACGCATGTATCTATC-3′ (5′-GPD) and 5′-TAATACGACTCACTATAGGG-3′ (T7). These primers complement the sequences upstream and downstream of the *E. coli Lep* gene in a plasmid. H1-10L/9A was generated by overlap PCR using the plasmid carrying the H1-1L/18A as a template. Two primers, 5′-GPD and 5′-CAGAGCTAGCGCGAGTGCCAAGGCTAGAGCCAGAGCTAAGGCTAATCCAGGACCACCACTAGT-3′ (RP24), were used to amplify the N-terminal part of the model protein. In a parallel reaction, two primers, 5′-CTGGCTCTAGCCTTGGCACTCGCGCTAGCTCTGGCCCTTGCACTTGGACCTGGTGGGGTACCG-3′ (RP23) and T7, were used for the amplification of the C-terminal part of the protein. Underlined sequences are complementary to sequences upstream and downstream of the hydrophobic segment (H-segment), and the rest are the complementary sequences coding for 10L/9A. The PCR products from both reactions were mixed and used as template in a second round of PCR using primers 5′-GPD and T7. Full-length PCR products were confirmed by sizing on an agarose gel and transformed into strain W303-1α (*MATα*, *ade2*, *can1*, *his3*, *leu2*, *trp1*, *ura3*) together with SmaI-linearized p424GPDHA. Yeast transformants were selected on −Trp plates. Plasmids were isolated, and the correct sequence was confirmed by DNA sequencing. All confirmed constructs were retransformed into BWY46, BWY497, and BWY500. Transformants were selected on −Trp plate and subjected to further analysis.

For construction of *SPC3HA*, *DAP2HA*, and *PHO8HA*, p424GPDHA vector was used as in the H1 model protein. The open reading frames of the genes were amplified using the following sets of primers: 5′-CCAGAACTTAGTTTCGACGGATTCTAGAACTAGTGGATCCATGTTCTCCTTTGTCCAAAGATTCCAGAATGTATCG-3′(5′-SPC3) and 5′-CGCATAGTCAGGAACATCGTATGGGTAAGATGGCTGCAGAACTTTGTTTTTATTTTCCACGGTCAGTGTATAGTTGCC-3′(3′-SPC3), 5′-CCAGAACTTAGTTTCGACGGATTCTAGAACTAGTGGATCCATGGAAGGTGGCGAAGAAGAAGTTGAGCGCATTCC-3′ (5′-DAP2) and 5′-CGCATAGTCAGGAACATCGTATGGGTAAGATGGCTGCAGTTTGACAAATTGCCCATCGAAAGCACGCTTTGCCCAATCC-3′ (3′-DAP2), 5′-CCAGAACTTAGTTTCGACGGATTCTAGAACTAGTGGATCCATGATGACTCACACATTACCAAGCGAACAGACACG-3′ (5′-PHO8) and 5′-CGCATAGTCAGGAACATCGTATGGGTAAGATGGCTGCAGATCTGATGTGTGTTTGGTGTCCCTAATCAAATCAGTGACTTCG-3′ (3′-PHO8), respectively, which contain homologous recombination sequences to p424GPDHA (underlined). The PCR products and SmaI-linearized p424GPDHA were transformed into yeast strain W303-1α and grown on −Trp plates, and then the correct sequences of isolated plasmids were confirmed by DNA sequencing. The hydrophobicity of the signal anchors of Dap2p and Pho8p was lowered by replacing hydrophobic residues with varying numbers of alanines by site-directed mutagenesis. Residues 202–720 of *DAP2HA* were deleted to facilitate separation by SDS-PAGE.

To generate a version of Spc3p that is inserted into the ER membrane as a dual topology and to aid detection of $N_{out}$-$C_{in}$ form of Spc3p, Q14K mutation, an *N*-glycosylation site ($^{3}$NST$^{5}$) and 4 residues ($^{8}$ESPA$^{11}$) at the N terminus were introduced by site-directed mutagenesis. The resulting construct, whose sequence was confirmed by DNA sequencing, was transformed into BWY46, BWY497, and BWY500 strains. The transformants were selected on −Trp plates and subjected to further analysis.

For construction of a set of plasmids carrying the *E. coli LepH1-HA-gGFP*, in the first step of PCR, each of the two plasmids carrying a gene for either *E. coli LepH1-HA* (11)or *E. coli yEGFP-E172T* (14) was amplified separately. *E. coli LepH1-HA* was amplified with primers 3N-LepGFPHR (CGACGGATTCTAGAACTAGTGGATCCATGGCGAATTCCACCAGC) and 3′-H2HA-GFP (AACACCAGTGAATAATTCTTCACCTTTAGAATTACATGACTCGAGGAG). 3N-LepGFPHR contains the homologous recombination sequence to the vector p424GPDHA, and 3′-H2HA-GFP contains overhang sequence complementing the start of the *yEGFP-E172T* sequence. *yEGFP-E172T* was amplified with primers 5′-H2HA-GFP (CCAGATTACGCTCTCCTCGAGTCATGTAATTCTAAAGGTGAAGA) and 3′-GFPendHR (ATCGATAAGCTTGATATCGAATTCCTGCAGTTATTTGTACAATTCATCCAT). 5′-H2HA-GFP contains the complementary sequence of the primer 3′-H2HA-GFP, and 3′-GFPendHR contains the *yEGFP-E172T* terminal sequence and the homologous recombination sequence to the vector, p424GPDHA. The second step of PCR was carried out using primers 3N-LepGFPHR and 3′-GFPendHR.

*Western Blot Analysis*—Yeast transformants carrying the H1 model protein constructs were grown in 5 ml of −Trp medium at 30 °C overnight, harvested by centrifugation at 3000 × *g*, washed with distilled $H_2O$, resuspended in 100 μl of SDS-PAGE sample buffer, heated for 15 min at 60 °C, and centrifuged down. The supernatant fractions were loaded onto 10% SDS gels and subsequently subjected to Western blotting using mouse anti-HA antiserum (Covance). For protein expression in the temperature-sensitive strains, BWY497 and BWY500, cells were grown at 23 °C overnight until an $A_{600}$ (absorbance at 600 nm) reached between 0.2 and 0.4 and incubated for another 4 h at 37 °C before harvesting. For endoglycosidase H (Endo H) digestion, 15 μl of the whole-cell lysate was mixed with 10.5 μl of distilled $H_2O$, 3 μl of Endo H buffer (800 mM sodium acetate, pH 5.8), and 1.5 μl of Endo H (5 units/ml; Roche Diagnostics) or distilled $H_2O$ for the mock treatment and incubated at 37 °C for 3 h.

*Pulse Labeling and Immunoprecipitation*—Cells for pulse labeling were either grown at 30 °C until an $A_{600}$ reached between 0.2 and 0.8 (BWY46) or grown at 23 °C until an $A_{600}$ of 0.1–0.3, and switched to 37 °C for additional 4 h (BWY46,

[3] The designations 1L, 2L, and so forth indicate sequences with one leucine, two leucines, and so forth. See Table 1 for sequences.

BWY497, and BWY500). Per reaction, 1.5 $A_{600}$ units of cells were harvested by centrifugation at 3000 × *g*, washed twice with −Met medium without ammonium sulfate, and incubated at 30 °C for 15 min or at 37 °C for 30 min. Cells were centrifuged and resuspended in 150 μl of −Met medium without ammonium sulfate and labeled with [$^{35}$S]Met (40 μCi/1.5 $A_{600}$ units of cells) for 5 min at 25 °C. Labeling was stopped by the addition of 750 μl of ice-cold stop solution buffer (20 mM Tris-HCl, pH 7.5, and 20 mM sodium azide). Cell pellets were harvested by centrifugation at 20,000 × *g* and left at −20 °C until further use. For pulse-chase experiments, radiolabeling was stopped and chased by the addition of 50 μl of 200 mM cold Met per 1.5 $A_{600}$ units of cells for 0, 5, or 15 min. The reaction was stopped by the addition of 750 μl of ice-cold stop solution buffer and centrifuged down, and cell pellets were kept frozen until use. Cell pellets were resuspended in 110 μl of lysis buffer (20 mM Tris-HCl, pH 7.5, 1% SDS, 1 mM DTT, 1 mM PMSF, and protease inhibitor mixture (Complete, Roche Applied Science)) and mixed with 100 μl of ice-cold acid-washed glass beads (Sigma). Cell suspensions were vortexed at maximum speed for 3 min. Then, samples were incubated at 60 °C for 15 min and centrifuged for 5 min at 20,000 × *g*. The supernatant fractions were mixed with 500 μl of immunoprecipitation (IP) buffer (15 mM Tris-HCl, pH 7.5, 0.1% SDS, 1% Triton X-100, and 150 mM NaCl), 1.3 μl of anti-HA antibody, and 50 μl of prewashed protein G-agarose beads (Roche Applied Science; 33% slurry in IP buffer) and rotated at 4 °C overnight. The agarose beads were washed twice with IP buffer, once with urea wash buffer (2 M urea, 200 mM NaCl, 10 mM Tris-HCl, pH 7.5, and 1% Triton X-100), once with ConA buffer (500 mM NaCl, 20 mM Tris-HCl, pH 7.5, and 1% Triton X-100), and once with buffer C (50 mM NaCl and 10 mM Tris-HCl, pH 7.5). Then, the beads were incubated with 55 μl of SDS-PAGE sample buffer at 60 °C for 15 min and centrifuged down, and the supernatant fractions were loaded onto SDS gels. Endo H treatment was carried out as described above. Radiolabeled bands on SDS gels were quantified using a Fuji FLA-3000 phosphorimaging device and the Image Reader V1.8J/Image Gauge version 3.45 software.

*Proteasome Inhibition*—Lep model protein was expressed in the *pdr5*Δ (*MATa*; *pdr5*Δ; *his3*Δ *1*; *leu2*Δ *0*; *met15*Δ *0*; *ura3*Δ *0*) strain. Cells were grown at 30 °C to an $A_{600}$ of 0.4–0.6. Three $A_{600}$ units per reaction were harvested and washed with 4.5 ml of −Met medium without ammonium sulfate and resuspended in 3 ml of the same buffer. The cell solution was split in two equal parts, added with 0.1 mM 132MG (Sigma) or the control buffer (DMSO), and incubated for 30 min at 30 °C. Cells were harvested, resuspended in 150 μl of −Met medium without ammonium sulfate, supplemented with 0.2 mM 132MG or DMSO, and subsequently labeled with 40 μCi of [$^{35}$S]Met. Pulse-Chase experiments and immunoprecipitation were carried out as described above.

## RESULTS

*Model Protein*—A modified *E. coli* Lep (11) was used as a model protein. The two N-terminal transmembrane (TM) domains of Lep were replaced by an engineered H-segment composed of varying numbers of Ala and Leu residues and flanked by *N*-linked glycosylation sites in the N (single site) and C (double sites) terminus (Fig. 1*A* and Table 1). If the Lep model protein is targeted and integrated into the ER membrane in $N_{out}$-$C_{in}$ membrane orientation, a singly glycosylated product (1G) is produced, whereas if it is integrated in $N_{in}$-$C_{out}$ membrane topology, a doubly glycosylated product (2G) is generated. Unglycosylated product represents nontranslocated Lep (0G) (Fig. 1*A*). Previously, it was shown that the H-segment could function both as a signal peptide and as a TM segment *in vitro* (11). For facilitating detection by IP or Western blotting, a triple hemagglutinin (HA) tag was fused to the C terminus of Lep. To identify the unglycosylated, nontranslocated product, samples prepared from a yeast transformant carrying the model protein with the 5L/14A H-segment were treated with Endo H, an enzyme that removes *N*-glycans (Fig. 1*B*).

*Defect in SRP Impairs Targeting of Signal Anchor Proteins of a Wide Range of Hydrophobicity, but Defect in Sec62 Impairs Moderately Hydrophobic Signal Anchor Proteins Only*—Although it is accepted that the targeting/translocation efficiency and routing preference are dependent on the degree of hydrophobicity of signal sequences, previous observations have been made with a limited number of protein substrates, such as carboxypeptidase Y, prepro-α-factor (ppαF), or dipeptidyl aminopeptidase B (Dap2) (8). To systematically evaluate the relationship between the hydrophobicity of the signal sequence and the targeting/translocation efficiency, we first expressed the Lep model protein carrying H-segments of varying hydrophobicity (containing 1L to 10L residues) in yeast WT (BWY46) cells and found that targeting efficiency is well correlated with the hydrophobicity of signal sequences (Fig. 1*C*).

Next, we investigated how the hydrophobicity governs the targeting route taken by the nascent chain by expressing Lep proteins carrying the H-segment of varying hydrophobicity in the temperature-sensitive yeast mutant strains defective in the SRP-dependent co-translational (BWY500/*sec65*) or the Sec62 dependent post-translational translocation (BWY497/*sec62*) (8, 15). Both strains are isogenic to the WT strain, BWY46. BWY500 carries mutations in *SEC65*, a gene encoding a subunit of SRP. BWY497 has a mutation in the N-terminal cytosolic domain of the Sec62, which is important for complex formation with Sec63 (16). It was reported that strains lacking functional SRP undergo physiological adaptation after 4 h of growth at nonpermissive temperature by slowing down translation (17). Hence, cells were grown overnight at low temperature (22 °C) and incubated at 37 °C only for 4 h followed by whole-cell lysate preparation, SDS-PAGE, and Western blotting.

In the SRP-defective strain (*sec65*), targeting and translocation efficiency dropped to ~20% for all signal sequences except 7L/12A (Fig. 2*A*). These results indicate that the capacity of SRP to recruit the signal anchor proteins to the ER rather than its interaction between the signal sequence was impaired in the *sec65* mutant strain. In comparison, in the Sec62-defective strain (*sec62*), only the model proteins carrying moderately hydrophobic signal sequences (3L to 5L, $\Delta G = -0.01$ to $-1.0$ kcal/mol) were impaired for targeting and translocation (Fig. 2*A*), indicating that Sec62 selectively mediates membrane insertion of moderately hydrophobic signal anchor proteins.

Next, we prepared a set of yeast signal anchor proteins with varying hydrophobicity. Spc3p, a subunit of signal peptidase

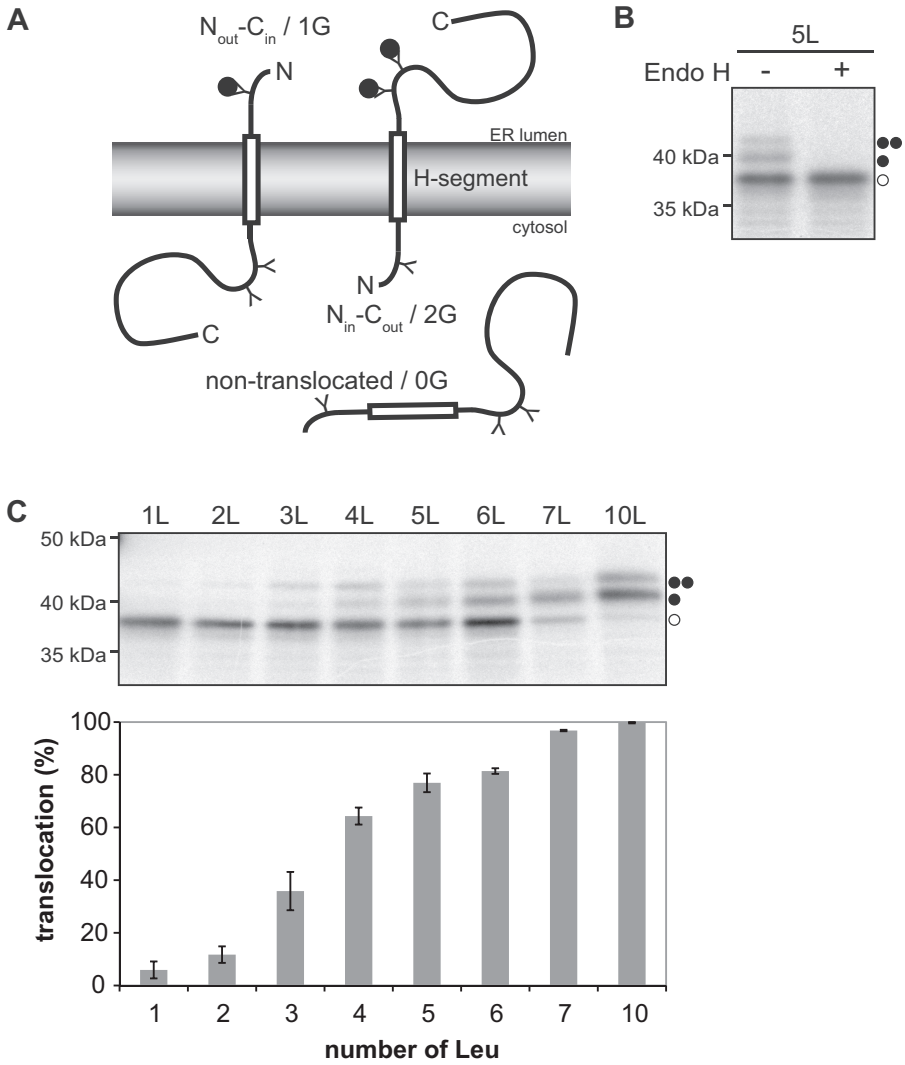


FIGURE 1. **Targeting and translocation of Lep model signal anchor protein with H-segment of varying hydrophobicity.** *A*, the *E. coli* Lep model protein contains a potential signal sequence (H-segment) composed of 19 residues of Ala and Leu (*white rectangle*) (Table 1). Three glycosylation sites are indicated as *Y*. If the model protein acquires an $N_{out}$-$C_{in}$ orientation, only the N-terminal glycosylation site is modified by the luminal oligosaccharyltransferase enzyme (*1G*), whereas the $N_{in}$-$C_{out}$ orientation leads to the doubly glycosylated form (*2G*). Nontranslocated protein remains unglycosylated (*0G*). *B*, yeast cells expressing the model protein containing a 5L/14A H-segment were labeled with [$^{35}$S]Met for 5 min, subjected to IP with an anti-HA antibody, subjected to SDS-PAGE, and analyzed by autoradiography. The samples were subjected to Endo H digestion or mock treatment prior to SDS-PAGE, as indicated. *Two filled circles* denote the 2G form, *one filled circle* denotes the 1G form, and *one open circle* denotes the 0G form of the model protein. The position of molecular mass markers is indicated in kilodaltons. *C,* model proteins with H-segments of varying hydrophobicity were expressed in WT (BWY46) cells. Whole-cell lysates were subjected to SDS-PAGE and Western blotting. Translocation efficiency (%) was calculated as the amount of glycosylated products over total products and was plotted against the number of Leu residues in the H-segment. Averages with S.E. of at least three independent measurements are shown. Labeling is as in *B*.

complex, contains a moderately hydrophobic signal anchor sequence (Table 1). Spc3p was expressed in WT and SRP (*sec65*)- and *sec62*-defective strains, and the ER targeting/translocation was assessed (Fig. 2*B*). Glycosylated products in both SRP (*sec65*)-defective and *sec62*-defective strains were reduced, indicating that targeting/translocation in the ER was impaired. Dap2p and Pho8p, a repressible alkaline phosphatase (18), contain very hydrophobic signal anchor sequences (Table 1). We prepared a set of Dap2p and Pho8p constructs carrying less hydrophobic signal anchor sequences by replacement of hydrophobic residue(s) with alanine to a range predicted to be influenced by Sec62 (between 2L and 5L) (Table 1). These constructs were expressed in WT and SRP (*sec65*)- and *sec62*-defective strains, and the efficiency of ER targeting/translocation was determined by assessing the amount of glycosylated products. Results show that when the hydrophobicity of Dap2p and Pho8p signal anchors is lowered, targeting and translocation are impaired in both SRP (*sec65*)-defective and *sec62*-defective strains (Fig. 2*B*). These results suggest that the SRP generally mediates targeting of signal anchor proteins to the ER, whereas Sec62 mediates translocation/membrane insertion of only those proteins carrying moderately hydrophobic signal anchor sequences.

*The Rate of Targeting and Translocation Differs Depending on the Hydrophobicity of Signal Anchor Sequences*—To investigate whether the rate of targeting and translocation depends on the hydrophobicity of signal sequences, the model protein with the H-segment composed of either 5L/14A or 10L/9A was radiolabeled with [$^{35}$S]Met for different periods of time. The model protein was subjected to IP with an anti-HA antibody

**TABLE 1**
**Summary of signal sequences used in this study**

| Protein | Signal sequence[a] | $\Delta G$[b] | Pathway model in this study |
|---|---|---|---|
| **1L** | AAAAAAAAALAAAAAAAA | 1.06 | SRP-independent |
| **2L** | AAAALAAAAAAAAALAAAA | 0.70 | SRP-independent |
| Pho8(3A) | KIIVSTVVCIG**AAA**VLVQLAF | 0.40 | SRP- and Sec62p-dependent |
| Spc3 | AFSMGIVMVVFIMASSYYQLI | 0.34 | SRP- and Sec62p-dependent |
| **3L** | AAAALAAAALAAAALAAAA | −0.01 | SRP- and Sec62p-dependent |
| Pho8(2A) | KIIVSTVVCIG**AA**LVLVQLAF | −0.11 | SRP- and Sec62p-dependent |
| Dap2(6A) | KLIRVG**AAA**VL**AAA**GTVLLL | −0.12 | SRP- and Sec62p-dependent |
| **4L** | AAAALALAAAAALALAAAA | −0.49 | SRP- and Sec62p-dependent |
| Pho8(A) | KIIVSTVVCIGL**A**LVLVQLAF | −0.74 | SRP- and Sec62p-dependent |
| Dap2(4A) | KLIRVGII**AAAA**IWGTVLLL | −0.87 | SRP- and Sec62p-dependent |
| **5L** | AAAALALAALAALALAAAA | −1.00 | SRP- and Sec62p-dependent |
| Pho8 | KIIVSTVVCIGLLLVLVQLAF | −1.13 | SRP- and Sec62p-dependent |
| **6L** | AAAALALALALALAAAA | −1.54 | SRP- and Sec62p-dependent |
| **7L** | ALAALALAALAALALAALA | −1.76 | SRP-dependent, Sec62p-independent |
| Dap2 | KLIRVGIILVLLIWGTVLLL | −2.93 | SRP-dependent, Sec62p-independent |
| **10L** | LALALALALALALALAL | −3.16 | SRP-dependent, Sec62p-independent |

[a] Signal sequences were predicted with SignalP 4.0 (34), except for Spc3 and Pho8. For the latter two, the TM segment acting as a signal sequence was predicted with $\Delta G$ predictor (35). Corresponding residues in Pho8 and Dap2 were changed to Ala (in boldface).
[b] $\Delta G$ values in kcal/mol were predicted with $\Delta G$ predictor.

and analyzed by SDS-PAGE and autoradiography (Fig. 3*A*). Although glycosylated product appeared within the first minute of labeling for the model protein carrying the 10L/9A H-segment, indicating simultaneous targeting and membrane insertion, the major product at shorter labeling times for the model protein containing the 5L/14A H-segment was an unglycosylated protein (Fig. 3*A*). To determine whether this unglycosylated product is eventually translocated, pulse-chase experiments were carried out. Yeast transformants expressing the model protein with the H-segment composition of 2L/15A, 5L/14A, or 10L/9A were radiolabeled with [$^{35}$S]Met for 5 min and chased for 0, 5, and 15 min (Fig. 3*B*). During the 15-min chase, glycosylated products of the model protein carrying the 2L/17A or 5L/14A H-segment were increased by ~30 and 50%, respectively, with concomitant decrease of unglycosylated product. To check whether unglycosylated product is converted to glycosylated products or is degraded in the cytosol, the model protein carrying the 5L/14A H-segment was expressed in the *pdr5*Δ strain (19) that is impaired in pumping out proteasome inhibitor (MG132) (Fig. 3*C*). By the 15-min chase, ~10% of unglycosylated products were detected for the cells untreated with MG132, whereas ~30% of unglycosylated products were detected for the cells treated with MG132 (Fig. 3*C*, *middle panel*), indicating that some unglycosylated products were degraded by the proteasome in the cytosol. However, glycosylated products were also increased by ~20 and ~30% with concomitant decrease of unglycosylated product in the 15-min chase for the cells untreated and treated with MG132, respectively, indicating that some unglycosylated products were slowly targeted to the ER and glycosylated (Fig. 3*C*, *right panel*). In the presence of MG132, more unglycosylated product was converted to glycosylated products during the 15-min chase, suggesting that when nontranslocated proteins are less degraded in the cytosol, they can be translocated slowly. Although *pdr5*Δ strain (19) is not isogenic to other strains used in this study, translocation and membrane insertion efficiency of the model protein in *pdr5*Δ strain in the absence of MG132 was comparable with the results with the WT strain. These results show that weakly/moderately hydrophobic signal sequences direct post-translational translocation at a slower rate, whereas strongly hydrophobic signal sequences guide co-translational translocation at a faster rate.

*Moderately Hydrophobic Signal Anchor Proteins Preferentially Acquire $N_{in}$-$C_{out}$ Membrane Topology*—Interestingly, the relative amount of doubly glycosylated product, corresponding to the model protein with $N_{in}$-$C_{out}$ membrane topology (Fig. 1*A*), was higher for moderately hydrophobic signal sequences (2L/17A = 74%, 5L/14A = 28%, at 0 min of chase) than the strongly hydrophobic signal sequence (10L/9A = 23% at 0 min of chase) (Fig. 4*A*, *left panel*). These results indicate that proteins that contain moderately hydrophobic signal anchor sequences may preferentially acquire $N_{in}$-$C_{out}$ (type II) membrane topology, whereas strongly hydrophobic signal anchor proteins insert more predominantly as $N_{out}$-$C_{in}$ (type I) membrane topology, which is consistent with findings by Wahlberg and Spiess (20)and Sakaguchi *et al.* (20, 21). During the 15-min chase, the relative amount of doubly glycosylated form ($N_{in}$-$C_{out}$ topology) was further increased, especially for the moderately hydrophobic signal sequence (5L/14A, from 27% to 54%) (Fig. 4*A*, *left panel*). However, the fraction of singly glycosylated product ($N_{out}$-$C_{in}$ membrane topology) changed little (Fig. 4*A*, *right panel*), indicating that slowly targeted nascent chains were preferentially integrated with an $N_{in}$-$C_{out}$ topology.

*Membrane Insertion of Moderately Hydrophobic Signal Sequences in $N_{in}$-$C_{out}$ (Type II) Topology Is Decreased in Sec62-defective Strain*—To test whether signal sequences acquire different membrane topology depending on the targeting route, a set of model proteins with H-segments of varying hydrophobicity was expressed in the *sec65* and *sec62* yeast mutant strains, and the fraction of signal sequences inserted with an $N_{in}$-$C_{out}$ topology was assessed by comparing the amount of doubly glycosylated product with that of singly glycosylated product (Fig. 4*B*). For the model protein carrying the 4L/15A or 5L/14A signal sequence, the amount of doubly glycosylated product was decreased more than 2-fold in the *sec62*-defective strain as compared with the WT or the SRP-defective strain (Fig. 4*B*). However, little or no change was observed when model proteins with the 6L/13A or 10L/9A signal sequence were expressed in the mutant strains. This suggests that Sec62 mediates mem-

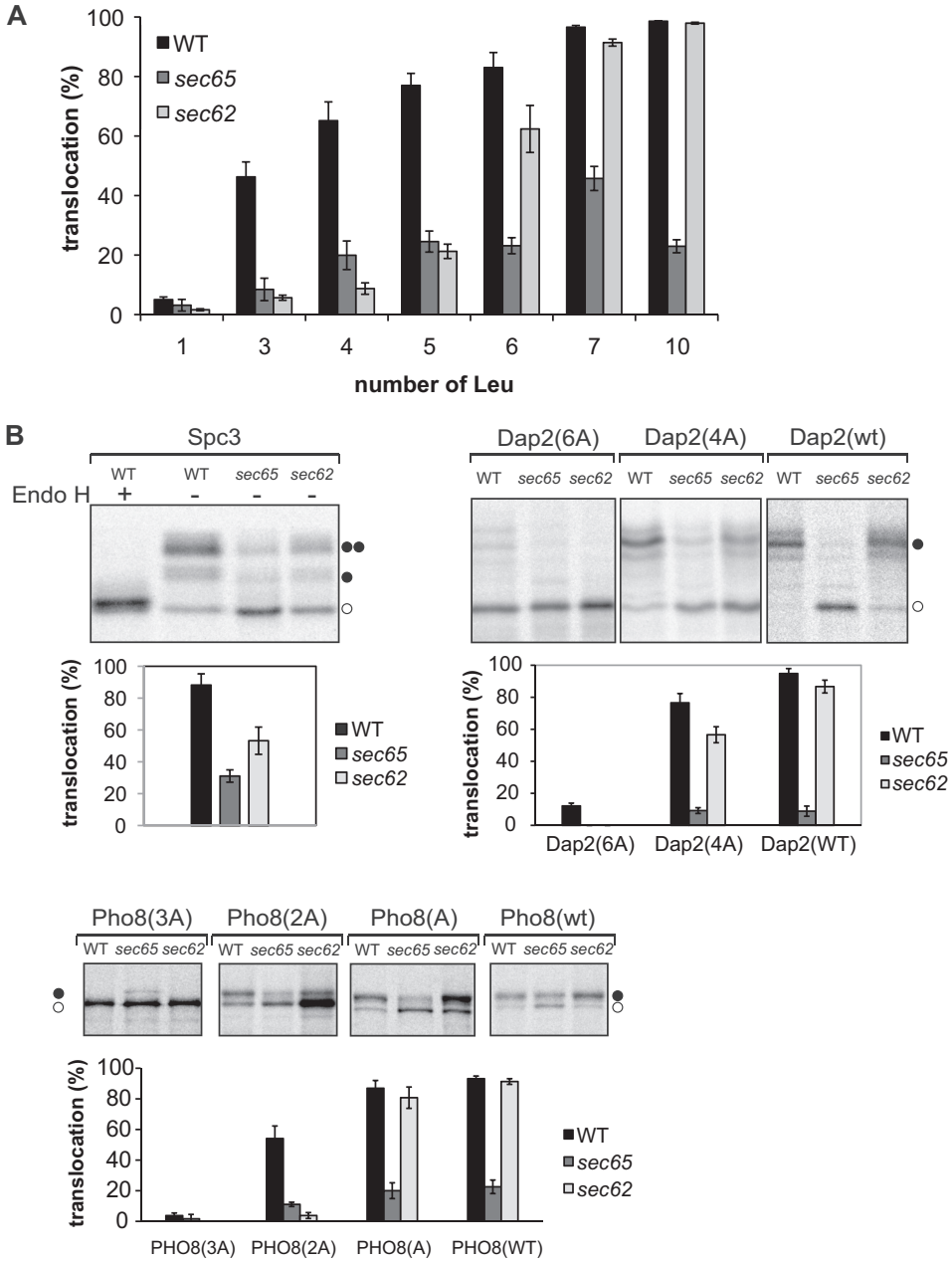


FIGURE 2. **Defective SRP impairs targeting of signal anchor proteins of a broad range of hydrophobicities, whereas defective Sec62 impairs moderately hydrophobic signal anchor proteins only.** *A*, translocation efficiency (%) of model proteins is plotted against the number of Leu residues in the H-segment. Model proteins carrying the H-segment of varying hydrophobicity were expressed in yeast wild type (*WT*, *black*) and conditional mutant strains, *sec65* (SRP-defective, *dark gray*) and *sec62* (Sec62-defective, *light gray*). Cells were grown at 22 °C overnight and switched to 37 °C for 4 h prior to whole-cell lysate preparation. Whole-cell lysates were subjected to SDS-PAGE and Western blotting with anti-HA antibody. Translocation efficiency was calculated as the amount of glycosylated products over the total amounts of the protein. Averages of at least three independent measurements with standard errors are shown. *B*, translocation efficiency of signal anchor proteins of varying hydrophobicity is shown. These proteins were labeled with [$^{35}$S]Met for 5 min, subjected to IP with anti-HA antibody, Endo H digestion, or mock treatment as indicated, subjected to SDS-PAGE, and analyzed by autoradiography.

brane insertion of moderately hydrophobic signal sequences as $N_{in}$-$C_{out}$ membrane topology.

*Defective Sec62 Reduces Membrane Insertion of Spc3p with $N_{in}$-$C_{out}$ Orientation*—In Fig. 2*B*, we observed that translocation of moderately hydrophobic signal anchor sequences of Dap2p and Pho8p and Spc3p was impaired in the *sec62*-defective strain. To test whether this defect is due to impaired translocation or membrane insertion of a signal anchor sequence as $N_{in}$-$C_{out}$ orientation by the Sec62, we prepared a version of Spc3p that inserts to the ER membrane with both $N_{in}$-$C_{out}$ and $N_{out}$-$C_{in}$ orientation by replacing Gln-21, which is located upstream of the TM domain, with Lys. It has been shown that positively charged flanking residues influence TM domain orientation according to the "positive-inside rule" (22). In addition to two natural glycosylation sites in the C terminus, a single *N*-linked glycosylation site was introduced at the N terminus (Fig. 4*C*). This asymmetric distribution of glycosylation sites allows us to monitor $N_{out}$-$C_{in}$ membrane orientation and gives the same glycosylation pattern as the Lep proteins. The targeting/translocation efficiency of this dual topology-competent

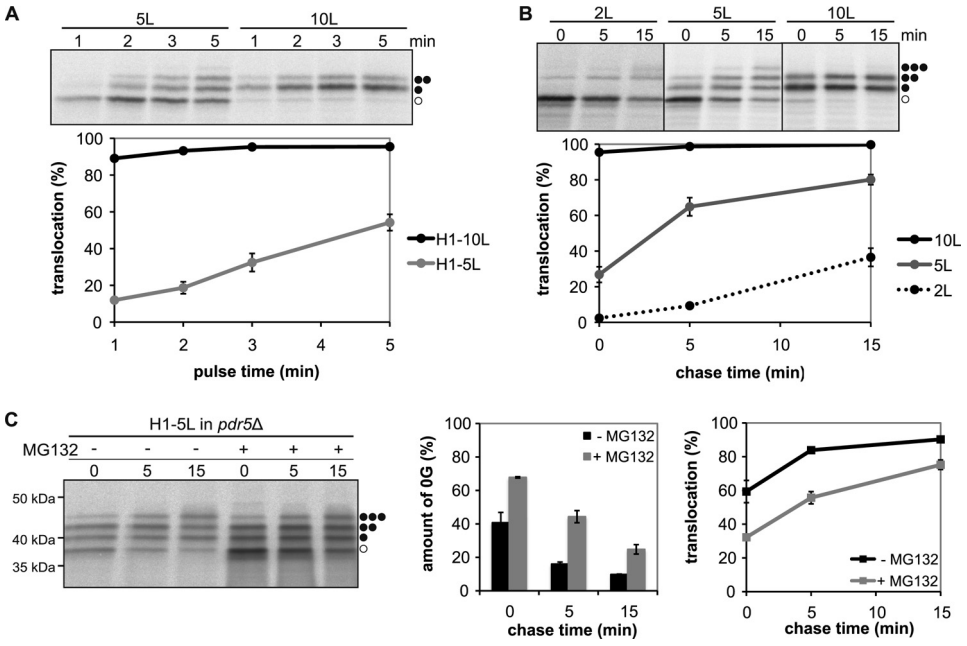


FIGURE 3. **The rate of targeting and translocation differs depending on the hydrophobicity of signal anchor sequences.** *A*, model proteins with an H-segment composed of 5L/14A or 10L/9L were labeled with [$^{35}$S]Met in wild type yeast cells for indicated times, subjected to IP with anti-HA antibody, subjected SDS-PAGE, and analyzed by autoradiography. Amounts of glycosylated proteins were quantified and plotted against the pulse time. *B*, model proteins with an H-segment composition of 2L/17A, 5L/14A, or 10L/9A were labeled with [$^{35}$S]Met in wild type yeast cells for 5 min and chased for 0, 5 and 15 min with cold Met. Samples were subjected to IP with anti-HA antibody, subjected to SDS-PAGE, and analyzed by autoradiography. The amount of glycosylated products was quantified and plotted against the chase time. *C*, for proteasome inhibition, *pdr5*Δ cells expressing the Lep model protein with an H-segment composition of 5L/14A were treated with MG132 or control buffer, as indicated (*left panel*). Samples were treated as in *B*. Amounts of unglycosylated and glycosylated proteins were quantified and plotted against the pulse time (*middle* and *right panel*, respectively; MG132, *black*; control buffer, *gray*). Averages of three independent measurements with S.D. are shown.

Spc3 (DT-Spc3p) is reduced in the mutant strains as compared with wild type. Of note, in all strains, the targeting/translocation efficiency of DT-Spc3p is higher than that of Lep model proteins of similar hydrophobicity (2L/17A and 3L/15A). We found that the relative amount of singly and doubly glycosylated DT-Spc3p is similar when expressed in WT strain. However, insertion of DT-Spc3p as $N_{in}$-$C_{out}$ orientation is decreased in the *sec62* mutant strain, whereas being minimally affected in the SRP mutant strain (Fig. 4*C*). These results suggest that translocation defect in *sec62* mutant strain may be due to impaired function of Sec62 in orienting the signal anchor sequence as $N_{in}$-$C_{out}$ orientation.

*Membrane Insertion of Moderately Hydrophobic Signal Sequences as $N_{in}$-$C_{out}$ Orientation Is Blocked with GFP Fusion at the C Terminus*—We reasoned that if moderately hydrophobic signal anchor proteins are post-translationally membrane inserted as $N_{in}$-$C_{out}$ orientation, tagging them with a green fluorescent protein (GFP) at the C terminus might prevent C-terminal translocation due to rapid and stable folding of the GFP, even in the wild type strain. We used a glycosylatable GFP (14), which folds correctly and fluoresces in the cytosol but loses fluorescence when glycosylated in the lumen. A set of model proteins carrying H-segments of varying hydrophobicity was tagged with a glycosylatable GFP (gGFP) and analyzed for translocation and membrane insertion (Fig. 4*D*, *left*). Translocation efficiency of GFP-tagged model proteins was greatly reduced for moderately hydrophobic signal sequences (3L-5L), whereas efficient translocation was observed for those with strongly hydrophobic signal anchor sequence (10L) in the wild type strain. (Fig. 4*D*, *middle*). In the *sec62* mutant strain, translocation efficiency of GFP-tagged model proteins was similar as in the wild type, but a complete block of translocation was observed in the *sec65* mutant strain (Fig. 4*D*). These results indicate that folding of GFP in the cytosol selectively prevents the Sec62-dependent post-translational translocation and membrane insertion of moderately hydrophobic signal sequences in an $N_{in}$-$C_{out}$ orientation.

## DISCUSSION

Our data suggest that signal anchor proteins are targeted to the ER membrane by the SRP, and if the signal anchor sequence is sufficiently hydrophobic, it is translocated co-translationally, independent of Sec62 (Fig. 5*A*). However, if the signal anchor sequence is weakly/moderately hydrophobic, it may be translocated post-translationally by the Sec62, mainly as $N_{in}$-$C_{out}$ (type II) membrane orientation (Fig. 5*B*).

It is unclear how the SRP targeted signal sequences are post-translationally translocated. One possibility is that the efficiency of translation arrest may differ. Although strongly hydrophobic signal sequences arrest translation effectively when bound to the SRP, moderately hydrophobic signal sequences may not efficiently arrest translation, allowing protein synthesis to continue. An earlier study by Plath and Rapoport (23) showed that ribosome-bound pp$\alpha$F, a post-translationally translocated protein, interacts with the SRP even when the nascent chain is almost full length. Further, Flanagan *et al.* (24) showed that SRP interaction with the signal sequence does not diminish as the nascent chain lengthens. These observa-

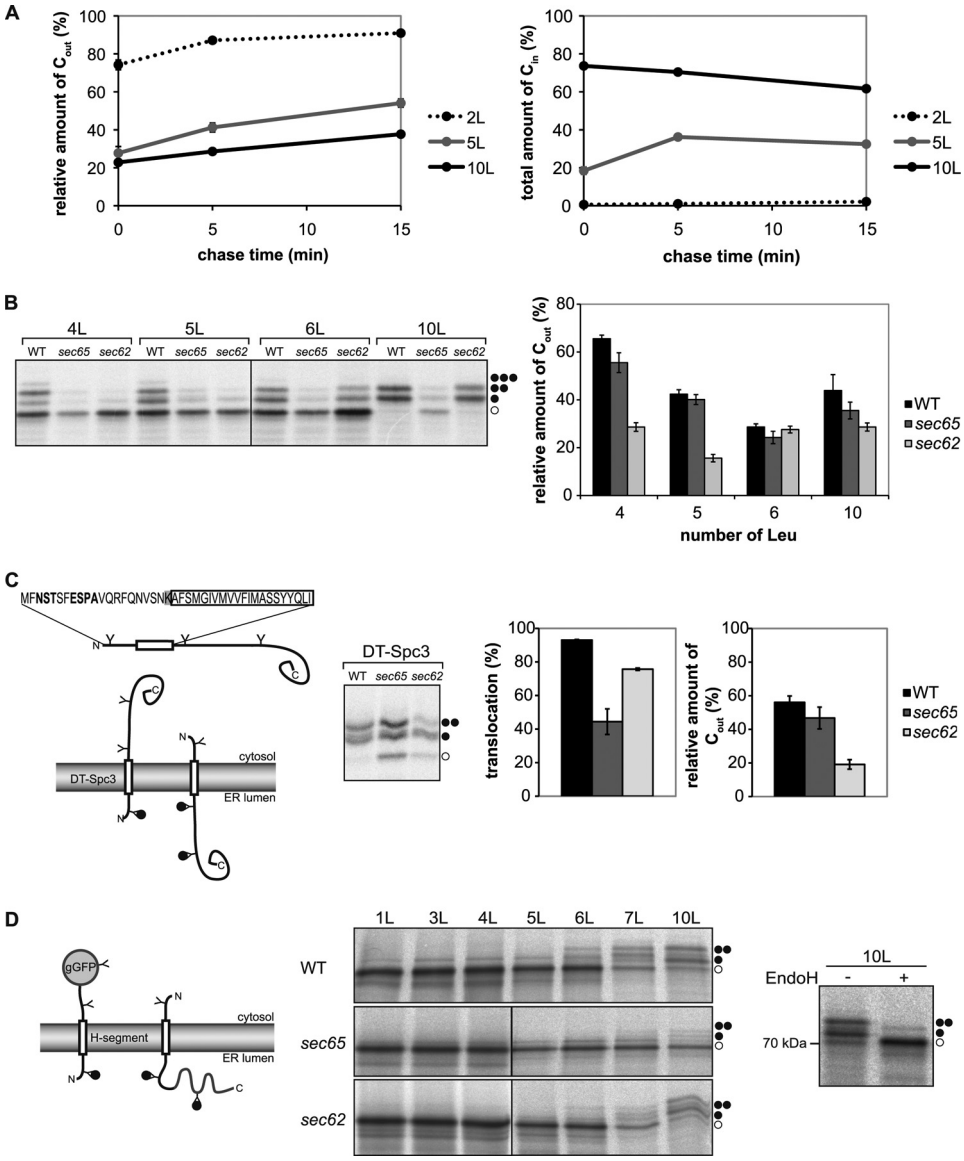


FIGURE 4. **Sec62 influences membrane insertion of moderately hydrophobic signal anchor sequences.** *A*, the relative amount of model proteins with $N_{in}$-$C_{out}$ membrane topology was quantified from the gel in Fig. 3*B* as (2G/(1G + 2G) × 100%) and plotted against the chase time (*left*). The total amounts of model proteins with $N_{out}$-$C_{in}$ membrane topology were quantified as (1G/(0G + 1G + 2G + 3G) × 100%) and plotted against the chase time (*right*). *B*, model proteins with the H-segment of the indicated sequence composition were expressed in yeast wild type (*WT*, *black*) and conditional mutant strains, *sec65* (SRP-defective, *dark gray*) and *sec62* (Sec62p-defective, *light gray*). Cells were grown overnight at 22 °C, switched to 37 °C for 4 h, labeled with [$^{35}$S]Met for 5 min at 25 °C, subjected to IP with anti-HA antibody, subjected to SDS-PAGE, and analyzed by autoradiography (*left*). The relative amount of model protein with $N_{in}$-$C_{out}$ membrane topology was calculated as (2G/(1G + 2G) × 100%) and plotted against the number of Leu residues in the H-segment (*right*). Averages of three independent measurements with standard errors are shown. *Three filled circles*, *two filled circles*, *one filled circle*, and *one open circle* denote triply, doubly, singly, and unglycosylated model proteins, respectively. *C*, schematic drawing of a dual topology-competent Spc3p (*DT-Spc3p*) and its N-terminal sequence containing the signal sequence (*boxed*), and the residues added (*bold*) and mutated (*shaded*), which are changes that promote Spc3p to insert in both orientations (*left*). DT-Spc3p was expressed in yeast wild type (*WT*, *black*) and conditional mutant strains, *sec65* (SRP-defective, *dark gray*) and *sec62* (Sec62p-defective, *light gray*). Samples were analyzed as in *B* (*right*). Averages with standard errors of at least three independent measurements are shown. *D*, a gGFP was fused to Lep model proteins of varying hydrophobicity (1L/18A-10L/9A) (*left*). GFP fusions were expressed in yeast wild type (WT) and conditional mutant strains, *sec65* (SRP-defective) and *sec62* (Sec62p-defective) (*middle*). Samples were treated as in *B*. GFP fusion protein with 10L/9A H-segment composition was subjected to Endo H digestion or mock treatment prior to SDS-PAGE (*right panel*). *Two filled circles* denote the 2G form, *one filled circle denotes* the 1G form, and *one open circle* denotes the 0G form of the model protein.

tions demonstrate that SRP binding to the signal sequence may not always lead to efficient translation arrest.

How signal sequences orient during insertion in the ER membrane has been controversial: loop insertion ($N_{in}$-$C_{out}$ topology) (25, 26) *versus* head-first insertion ($N_{out}$-$C_{in}$ topology) (20, 22, 27–31). We present data that the Sec62 mediates membrane insertion of moderately hydrophobic signal anchor sequences preferentially in an $N_{in}$-$C_{out}$ (type II) topology. Earlier cross-linking studies (25, 32) have shown that the signal sequence of pp$\alpha$F became concomitantly cross-linked with the Sec61 gating helices, TM2/TM7 and Sec62, suggesting that the Sec62 is in close proximity to the gating helices of Sec61 where the TM segment of a nascent chain exits to the membrane. Interestingly, when the shorter cross-linker was used, the Sec62 was cross-linked only when the probe was incorporated into the C-terminal end of the signal sequence of pp$\alpha$F

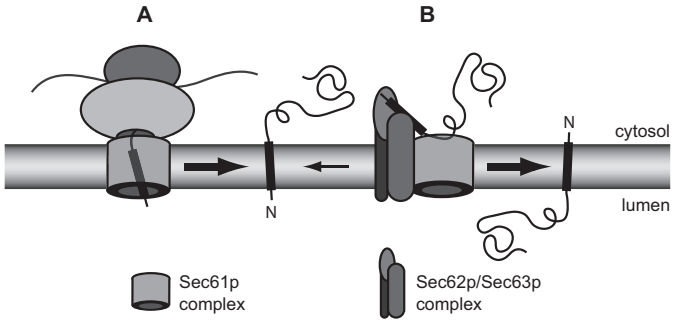


FIGURE 5. **Proposed model for targeting of a signal anchor protein to the ER.** When a sufficiently hydrophobic segment of a nascent chain emerges from the ribosome, it is tightly bound by the SRP, targeted to the ER membrane, and co-translationally translocated through the Sec61 translocon (*A*). For moderately hydrophobic signal anchor proteins, a nascent chain is targeted by the SRP and resorted by the Sec62/63 complex at the ER membrane (*B*). Sec62 mediates membrane insertion of a signal anchor proteins preferentially in $N_{in}$-$C_{out}$ orientation.

(25). Based on these earlier observations and our data, it is tempting to speculate that moderately hydrophobic signal sequences may linger at the lateral exit site of the Sec61 for longer as compared with more hydrophobic ones, and thus increase the probability of interacting with Sec62. Another potential mechanism would be a direct recognition of moderately hydrophobic segments by the Sec62 as part of the targeting process of post-translational translocation (33). Once recognized, the Sec62 would help position the C-terminal end of the signal sequence in the luminal side of the ER membrane. We expect this to apply to both signal anchor and cleavable signal sequences, for which the $N_{in}$-$C_{out}$ orientation is essential for cleavage by the signal peptidase in the luminal side of the ER membrane. Although detailed molecular mechanisms remain elusive at present, we report data that suggest a previously unknown role of the Sec62 in regulating the orientation of signal anchor sequences in an early stage of translocation in the ER.

*Acknowledgments—We thank Drs. Barry Wilkinson, Colin Stirling (University of Manchester, United Kingdom), and Tadashi Sukuzi (RIKEN Institute, Saitama, Japan) for yeast strains, Chewon Yim for construction of plasmids carrying gGFP, and laboratory members for critical reading of the manuscript.*

## REFERENCES

1. Rapoport, T. A. (2007) Protein translocation across the eukaryotic endoplasmic reticulum and bacterial plasma membranes. *Nature* **450,** 663–669
2. Panzner, S., Dreier, L., Hartmann, E., Kostka, S., and Rapoport, T. A. (1995) Posttranslational protein transport in yeast reconstituted with a purified complex of Sec proteins and Kar2p. *Cell* **81,** 561–570
3. Matlack, K. E., Misselwitz, B., Plath, K., and Rapoport, T. A. (1999) BiP acts as a molecular ratchet during posttranslational transport of prepro-α factor across the ER membrane. *Cell* **97,** 553–564
4. Lakkaraju, A. K., Thankappan, R., Mary, C., Garrison, J. L., Taunton, J., and Strub, K. (2012) Efficient secretion of small proteins in mammalian cells relies on Sec62-dependent posttranslational translocation. *Mol. Biol. Cell* **23,** 2712–2722
5. Meyer, H. A., Grau, H., Kraft, R., Kostka, S., Prehn, S., Kalies, K. U., and Hartmann, E. (2000) Mammalian Sec61 is associated with Sec62 and Sec63. *J. Biol. Chem.* **275,** 14550–14557
6. Tyedmers, J., Lerner, M., Bies, C., Dudek, J., Skowronek, M. H., Haas, I. G., Heim, N., Nastainczyk, W., Volkmer, J., and Zimmermann, R. (2000) Homologs of the yeast Sec complex subunits Sec62p and Sec63p are abundant proteins in dog pancreas microsomes. *Proc. Natl. Acad. Sci. U.S.A.* **97,** 7214–7219
7. Müller, L., de Escauriaza, M. D., Lajoie, P., Theis, M., Jung, M., Müller, A., Burgard, C., Greiner, M., Snapp, E. L., Dudek, J., and Zimmermann, R. (2010) Evolutionary gain of function for the ER membrane protein Sec62 from yeast to humans. *Mol. Biol. Cell* **21,** 691–703
8. Ng, D. T., Brown, J. D., and Walter, P. (1996) Signal sequences specify the targeting route to the endoplasmic reticulum membrane. *J. Cell Biol.* **134,** 269–278
9. Lee, H. C., and Bernstein, H. D. (2001) The targeting pathway of *Escherichia coli* presecretory and integral membrane proteins is specified by the hydrophobicity of the targeting signal. *Proc. Natl. Acad. Sci. U.S.A.* **98,** 3471–3476
10. Wilkinson, B. M., Tyson, J. R., and Stirling, C. J. (2001) Ssh1p determines the translocation and dislocation capacities of the yeast endoplasmic reticulum. *Dev. Cell* **1,** 401–409
11. Lundin, C., Kim, H., Nilsson, I., White, S. H., and von Heijne, G. (2008) Molecular code for protein insertion in the endoplasmic reticulum membrane is similar for $N_{in}$-$C_{out}$ and $N_{out}$-$C_{in}$ transmembrane helices. *Proc. Natl. Acad. Sci. U.S.A.* **105,** 15702–15707
12. Ho, S. N., Hunt, H. D., Horton, R. M., Pullen, J. K., and Pease, L. R. (1989) Site-directed mutagenesis by overlap extension using the polymerase chain reaction. *Gene* **77,** 51–59
13. Oldenburg, K. R., Vo, K. T., Michaelis, S., and Paddon, C. (1997) Recombination-mediated PCR-directed plasmid construction *in vivo* in yeast. *Nucleic Acids Res.* **25,** 451–452
14. Lee, H., Min, J., von Heijne, G., and Kim, H. (2012) Glycosylatable GFP as a compartment-specific membrane topology reporter. *Biochem. Biophys. Res. Commun.* **427,** 780–784
15. Stirling, C. J., Rothblatt, J., Hosobuchi, M., Deshaies, R., and Schekman, R. (1992) Protein translocation mutants defective in the insertion of integral membrane proteins into the endoplasmic reticulum. *Mol. Biol. Cell* **3,** 129–142
16. Wittke, S., Dünnwald, M., and Johnsson, N. (2000) Sec62p, a component of the endoplasmic reticulum protein translocation machinery, contains multiple binding sites for the Sec-complex. *Mol. Biol. Cell* **11,** 3859–3871
17. Mutka, S. C., and Walter, P. (2001) Multifaceted physiological response allows yeast to adapt to the loss of the signal recognition particle-dependent protein-targeting pathway. *Mol. Biol. Cell* **12,** 577–588
18. Klionsky, D. J., and Emr, S. D. (1989) Membrane protein sorting: biosynthesis, transport and processing of yeast vacuolar alkaline phosphatase. *EMBO J.* **8,** 2241–2250
19. Collins, G. A., Gomez, T. A., Deshaies, R. J., and Tansey, W. P. (2010) Combined chemical and genetic approach to inhibit proteolysis by the proteasome. *Yeast* **27,** 965–974
20. Wahlberg, J. M., and Spiess, M. (1997) Multiple determinants direct the orientation of signal-anchor proteins: the topogenic role of the hydrophobic signal domain. *J. Cell Biol.* **137,** 555–562
21. Sakaguchi, M., Tomiyoshi, R., Kuroiwa, T., Mihara, K., and Omura, T. (1992) Functions of signal and signal-anchor sequences are determined by the balance between the hydrophobic segment and the N-terminal charge. *Proc. Natl. Acad. Sci. U.S.A.* **89,** 16–19
22. Goder, V., and Spiess, M. (2003) Molecular mechanism of signal sequence orientation in the endoplasmic reticulum. *EMBO J.* **22,** 3645–3653
23. Plath, K., and Rapoport, T. A. (2000) Spontaneous release of cytosolic proteins from posttranslational substrates before their transport into the endoplasmic reticulum. *J. Cell Biol.* **151,** 167–178
24. Flanagan, J. J., Chen, J. C., Miao, Y., Shao, Y., Lin, J., Bock, P. E., and Johnson, A. E. (2003) Signal recognition particle binds to ribosome-bound signal sequences with fluorescence-detected subnanomolar affinity that does not diminish as the nascent chain lengthens. *J. Biol. Chem.* **278,** 18628–18637
25. Plath, K., Mothes, W., Wilkinson, B. M., Stirling, C. J., and Rapoport, T. A. (1998) Signal sequence recognition in posttranslational protein transport across the yeast ER membrane. *Cell* **94,** 795–807

26. Shaw, A. S., Rottier, P. J., and Rose, J. K. (1988) Evidence for the loop model of signal-sequence insertion into the endoplasmic reticulum. *Proc. Natl. Acad. Sci. U.S.A.* **85,** 7592–7596
27. Devaraneni, P. K., Conti, B., Matsumura, Y., Yang, Z., Johnson, A. E., and Skach, W. R. (2011) Stepwise insertion and inversion of a type II signal anchor sequence in the ribosome-Sec61 translocon complex. *Cell* **146,** 134–147
28. Eusebio, A., Friedberg, T., and Spiess, M. (1998) The role of the hydrophobic domain in orienting natural signal sequences within the ER membrane. *Exp. Cell Res.* **241,** 181–185
29. Rösch, K., Naeher, D., Laird, V., Goder, V., and Spiess, M. (2000) The topogenic contribution of uncharged amino acids on signal sequence orientation in the endoplasmic reticulum. *J. Biol. Chem.* **275,** 14916–14922
30. Spiess, M. (1995) Heads or tails–what determines the orientation of proteins in the membrane. *FEBS Lett.* **369,** 76–79
31. Kocik, L., Junne, T., and Spiess, M. (2012) Orientation of internal signal-anchor sequences at the Sec61 translocon. *J. Mol. Biol.* **424,** 368–378
32. Plath, K., Wilkinson, B. M., Stirling, C. J., and Rapoport, T. A. (2004) Interactions between Sec complex and prepro-α-factor during posttranslational protein transport into the endoplasmic reticulum. *Mol. Biol. Cell* **15,** 1–10
33. Heinrich, S. U., Mothes, W., Brunner, J., and Rapoport, T. A. (2000) The Sec61p complex mediates the integration of a membrane protein by allowing lipid partitioning of the transmembrane domain. *Cell* **102,** 233–244
34. Petersen, T. N., Brunak, S., von Heijne, G., and Nielsen, H. (2011) SignalP 4.0: discriminating signal peptides from transmembrane regions. *Nat. Methods* **8,** 785–786
35. Hessa, T., Meindl-Beinker, N. M., Bernsel, A., Kim, H., Sato, Y., Lerch-Bader, M., Nilsson, I., White, S. H., and von Heijne, G. (2007) Molecular code for transmembrane-helix recognition by the Sec61 translocon. *Nature* **450,** 1026–1030